

Heterogeneous Photocatalytic Click Chemistry

Bowen Wang,^{†,‡,§} Javier Durantini,^{†,§} Jun Nie,^{*,‡} Anabel E. Lanterna,^{*,†} and Juan C. Scaiano^{*,†}

[†]Department of Chemistry and Biomolecular Sciences and Centre for Catalysis Research and Innovation, University of Ottawa, Ottawa, Ontario, Canada K1N 6N5

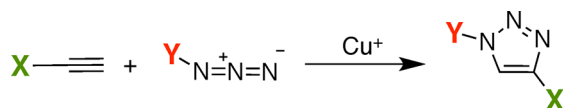
[‡]State Key Laboratory of Chemical Resource Engineering, Faculty of Science, Beijing University of Chemical Technology, Beijing 100029, China

S Supporting Information

ABSTRACT: Copper-doped semiconductors are designed to photoassist the alkyne–azide cycloaddition catalysis by Cu(I). Upon irradiation, injection of electrons from the semiconductor into copper oxide nanostructures produces the catalytic Cu(I) species. The new catalysts are air- and moisture-tolerant and can be readily recovered after use and reused several times.

Click chemistry (as in Scheme 1) is typically a thermal process efficiently catalyzed by Cu(I)¹ or copper

Scheme 1. Copper-Catalyzed Azide–Alkyne Cycloaddition Reaction (CuAAC)



nanostructures.² In a recent publication, we demonstrated that the process involves “truly” heterogeneous catalysis³ as opposed to examples where heterogeneous systems act as suppliers for soluble catalysts; in such cases, the advantages of heterogeneous chemistry are defeated by the leaching of active materials.⁴ A commercial copper-on-charcoal catalyst is also available for click chemistry,⁵ which in spite of its usefulness in organic chemistry contains less than 0.003% active surface.⁶ Here we report a heterogeneous photoactivated catalyst for the click reaction, specifically for the Huisgen cycloaddition of azides and terminal alkynes. Furthermore, this makes catalyst separation and reuse straightforward. In fact, there have been a few interesting reports of “photo-click” chemistry. Some of them involve photoactivation of an organic reagent,⁷ while others use organic photoreducing agents to convert soluble Cu(II) to Cu(I), the active catalyst.^{8,9} The latter approach can afford more flexibility, as it could be largely independent of the detailed structure of the substrates. The use of light combined with reusable heterogeneous catalysts reduces adverse environmental effects and thus accommodates some of the key strategies of green chemistry.

In this contribution, we report that semiconductors with band gaps within the 3–3.5 eV range (e.g., TiO₂ and Nb₂O₅) decorated with CuO_x nanostructures serve as effective photoactivated click catalysts. Earlier reports include a catalyst with copper hydroxide supported on alumina and titanium oxide,¹⁰

but in that case thermal click reactions required a temperature of 60 °C under an oxygen-free atmosphere. Other articles describe applications of Cu on TiO₂ for water splitting,¹¹ CO₂ photoreduction, or biomedical research¹² but, to the best of our knowledge, not to photoinitiated catalytic organic reactions. In a related article, Bowman and co-workers⁹ explored the use of suspended TiO₂ to reduce Cu(II) in solution; while the system worked, it was dismissed as impractical for the imaging applications under study. In a recent review, Pale and co-workers covered numerous methods involving heterogeneous catalysis of click chemistry that have been or are currently being developed;¹³ surprisingly, none of them involves photoactivated catalysis.

This work was undertaken with the goal of developing a hybrid catalyst, as illustrated in Figure 1 for TiO₂ (it is similar

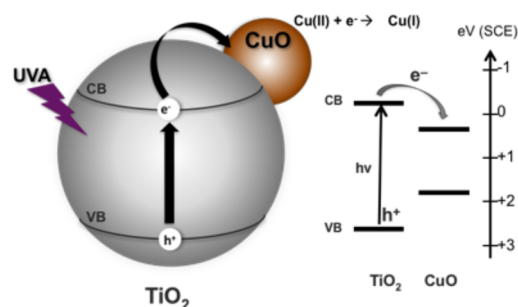


Figure 1. Proposed mechanism of electron transfer from the excited semiconductor to CuO nanoparticles to form catalytic Cu(I).

for Nb₂O₅) decorated with copper nanoparticles, mainly present as oxides (vide infra). When CuO is supported on TiO₂, its conduction band is about 0.3 eV lower than that of TiO₂ (the exact gap depends on the particle size), making the electron transfer shown quite favorable.¹⁴ For both semiconductors, excitation in the band gap region (normally in the UVA region, see Figure S1) promotes a valence band electron to the conduction band. Under normal circumstances, electron–hole recombination is a relatively fast process unless either the electron or hole is trapped; in our case, CuO on the surface can trap the electron, yielding Cu(I) (Figure 1).^{12,14–16} Electron donors can trap the hole and in the process hinder the recombination; amines and alcohols can perform this role (vide

Received: July 5, 2016

Published: September 27, 2016

infra). In other systems, the electron can be trapped by O_2 and the hole by water in well-understood processes, particularly in the case of TiO_2 ,^{12,17} although there are also a few examples involving Nb_2O_5 .^{16,18} There are examples¹² where, taking advantage of the reduced recombination rates, the electron, the hole, or both are trapped by species in solution, including the solvent itself.¹⁴ The quantum yields of these processes are limited to <1 , as one photon can cause only one electron to be promoted and at best one chemical change can take place involving the surface of these materials. In our system the effect of excitation is amplified, as photoexcitation leads to the generation of one catalytic site on the surface (i.e., a Cu(I) site) that is capable of multiple catalytic events until recombination inexorably takes place.

In order to test the validity of our hypothesis, we prepared $CuO_x@TiO_2$ and $CuO_x@Nb_2O_5$ and used the reaction between **1a** and **2a** as a model system (Table 1). The synthesis of nanoparticles decorating the semiconductors was achieved in situ using benzoin I-2959 as a source of reducing ketyl radicals, as shown in Scheme S1.¹⁹ This normally produces the metal nanoparticles, and in the case of copper, air exposure oxidizes them to CuO, a process that has been characterized earlier.¹⁴ The early generation of low oxidation states of copper (Cu(0) or Cu(I)) is clearly evidenced by the brownish color of the materials, which in the case of TiO_2 is only visible before the samples are exposed to air, after which they turn to light gray, characteristic of supported CuO (Figure S2). The X-ray photoelectron spectroscopy (XPS) spectrum of $CuO_x@TiO_2$ shows the characteristic satellite peaks of Cu(II)²⁰ between 945 and 940 eV, further confirming the presence of CuO. In the case of $CuO_x@Nb_2O_5$, more reduced Cu species are present initially (Figure S3), although differentiation between Cu(I) and Cu(0) is not accurate by this technique.²¹ Cu(I), if present, was below the limit of detection of our Raman spectrometer. The Cu loadings were determined by inductively coupled plasma optical emission spectroscopy (ICP-OES) analysis and found to be 2.51 and 2.04 wt % for $CuO_x@Nb_2O_5$ and $CuO_x@TiO_2$, respectively. Analysis of scanning electron microscopy (SEM) and scanning transmission electron microscopy (STEM) images indicated that the nanoparticles deposited on TiO_2 were considerably smaller than those on Nb_2O_5 (see the SI).

In order to evaluate the efficiency of the photocatalytic activity of $CuO_x@Nb_2O_5$ for CuAAC, a series of experiments were performed to optimize the reaction conditions (Table 1). The reaction was tested with different polar solvents and to compare the use of amines and alcohols as cocatalysts. For most CuAAC reactions, the addition of amines is anticipated to protect and stabilize copper(I) from oxidation.^{13,22} We believe the main role of the amine here is to act as a hole scavenger, and hence, the reaction is expected to work with other sacrificial electron donors (EDs). Indeed, for $CuO_x@Nb_2O_5$ the reaction works very well when amine is replaced by 2-propanol, although the same is not true for $CuO_x@TiO_2$, where the effectiveness of alcohol as a hole scavenger is inferior (Figure S9). There are literature precedents showing the superior catalytic activity of Nb_2O_5 toward alcohol oxidation.²³ Experiments performed in the absence of an ED can also lead to good yields, although the reaction rate decreases, as shown in Figures 2 and S12. Control experiments in the absence of catalyst or in the presence of TiO_2 or Nb_2O_5 were also performed, but no click reaction was detected.

Table 1. Effect of the Solvent and the Electron Donor (ED) on the Photocatalytic CuAAC Using $CuO_x@Nb_2O_5$ as the Catalyst^a

entry	solvent	ED	% yield of 3a	
			light ^b	dark
1	CH ₃ CN	TEA	28	5
2	H ₂ O	TEA	35	4
3	EtOH	TEA	34	5
4	THF	TEA	90	15
5	THF	PMDTA	83	13
6	THF	2-propanol ^c	96	4
7	THF	none	58	ND

^aReaction conditions: Cu (1.2 mol %), azide/alkyne/ED (1:1:1), room temperature, 6 h. Abbreviations: PMDTA, *N,N',N'',N'''*-pentamethyldiethylenetriamine; TEA, triethylamine. Yields were calculated by ¹H NMR analysis in CDCl₃. ^bUVA irradiation at 21.4 W/m². ^c5 mmol.

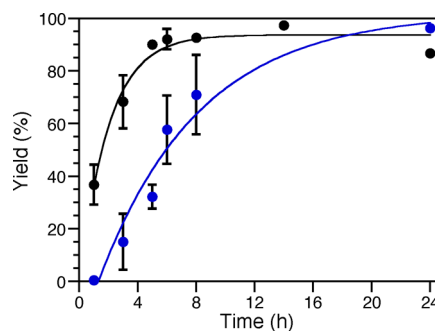


Figure 2. Kinetic study of the photocatalytic reaction of **1a** and **2a** in THF in the presence (black) or absence (blue) of TEA using $CuO_x@Nb_2O_5$ as the photocatalyst.

Overall, the reaction conditions that best suit both materials (Table 1, entry 4, and Figure S9) were chosen to study their catalytic activity. The kinetic study of the reaction between **1a** and **2a** is shown in Figure 3. Interestingly, under dark conditions the catalysts show slightly different activities; $CuO_x@TiO_2$ is inactive, while $CuO_x@Nb_2O_5$ shows a small but non-negligible amount of products, probably as a result of the nature of the catalytic copper species present in the latter. The presence of some reduced Cu species, as confirmed by

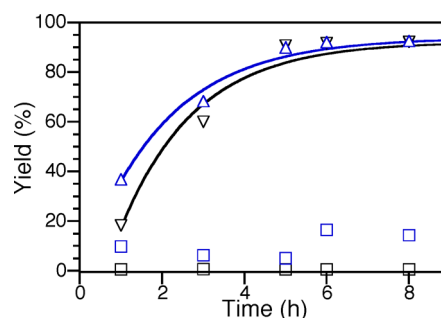


Figure 3. Kinetic study of the photocatalytic reaction of **1a** and **2a** in THF in the dark (\square) and upon UVA irradiation (Δ and ∇). Black: $CuO_x@TiO_2$. Blue: $CuO_x@Nb_2O_5$.

XPS analysis, should favor some reaction under dark conditions for $\text{CuO}_x@\text{Nb}_2\text{O}_5$. Both catalysts reach ca. 90% yield after 5 h of UVA irradiation. If the light is turned off, the catalysis yields are reduced, suggesting that transient Cu(I) needs continued irradiation for its activity level to be maintained (Figure 4). Although greatly reduced, some reactivity remains for some time after the light is turned off.

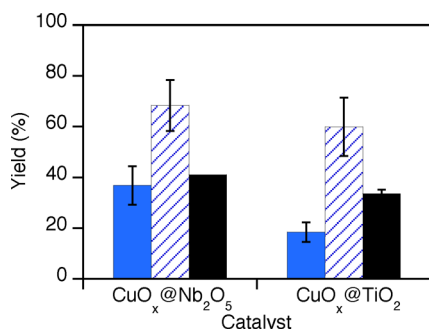


Figure 4. Yields obtained for each material after irradiation for 1 h (blue), 3 h (blue striped), and 1 h followed by 2 h in the dark (black). For $\text{CuO}_x@\text{TiO}_2$, a 16% yield was produced in the dark after UV exposure, while for $\text{CuO}_x@\text{Nb}_2\text{O}_5$ the value was within experimental error.

We were surprised to discover that a “control” experiment at 525 nm led to click products, albeit in yields after 4 h that were about 4 times lower than for excitation at 368 nm. This inspired exploratory experiments performed at longer wavelengths (594, 660, and 740 nm). With the exception of excitation at 740 nm, all of these wavelengths caused reaction, even after just 4 h, although with decreasing yields at the longer wavelengths. This is summarized in Table S1. Control experiments at 525 nm showed that CuO and Cu_2O have no photocatalytic activity (see Table S1). The lack of activity showed by Cu_2O may be due to the small surface area available and CuO contamination (see Figures S7 and S8). We speculate that under visible-light irradiation, absorption by the smaller (and thus larger band gap) CuO particles leads to oxide-mediated electron transfer to larger CuO particles, while the hole ultimately resides in the oxide support. This electron shuttle, which is illustrated in Figure S11 for $\text{CuO}_x@\text{TiO}_2$, leads to Cu(I) in the larger CuO particles. Interestingly, in the mechanism proposed, polydispersity ultimately helps the photocatalytic process. The practical result is that the catalysts can be activated with visible light and provide wavelength tunability of the light-induced CuAAC reaction without the use of organic photoinitiators.²⁴

Interestingly, under argon the reaction stops at half of its normal yield (Figures 5 and S12). Opening the vessel after the plateau is reached leads to an increase in the reaction yield to almost 90% within 2 h of irradiation. This is likely due to over-reduction of the catalyst to Cu(0). The presence of O_2 may play a role in the oxidation of both Cu(I) and Cu(0) to keep the catalytic cycle active, as shown in the inset of Figure 5.²¹

Table 2 shows a study of the scope of this reaction with respect to the alkyne and the azide (Chart 1). Both catalysts show great versatility toward phenyl alkynes substituted with electron-donating or electron-withdrawing groups at the para position, although TiO_2 seems to work slightly better than Nb_2O_5 with ortho-substituted reactants. Furthermore, the reaction can be extended for use with aliphatic alkynes, with TiO_2 being quite effective, even with bulky reactants (cf. entries

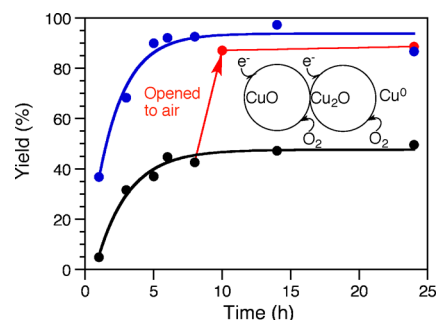


Figure 5. Study of the photocatalytic reaction of **1a** and **2a** in THF in Ar (black) or air (blue) using $\text{CuO}_x@\text{Nb}_2\text{O}_5$. The red dots show the yields obtained when the system was exposed to air after 8 h of reaction under Ar. Inset: role of O_2 in the Cu redox cycle.

Table 2. Scope of the Photocatalytic CuAAC^a

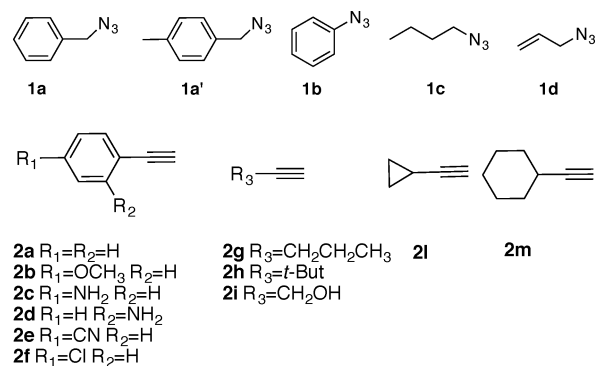
$$\text{R-N}_3 + \text{R}'\text{-C}\equiv\text{C} \xrightarrow[\text{THF, air}]{\text{CuO}_x@\text{support}, \text{TEA}} \text{R}'\text{-C}\equiv\text{C-N}_2\text{-R}$$

1 2 3

entry	time (h)	reactants ^b	support	
			Nb_2O_5	TiO_2
1	6	1a , 2a	>99	92
2	6	1a' , 2a	93	>99
3	6	1b , 2a	ND	ND
4	6	1c , 2a	78	89
5	24	1d , 2a	92	72
6	8	1a , 2b	90	89
7	24	1a , 2c	67	59
8	24	1a , 2d	41	58
9	24	1a , 2e	66	75
10	6	1a , 2f	79	80
11	24	1a , 2g	68	86
12	6	1a , 2h	6	60
13	24	1a , 2i	81	82
14	6	1a , 2l	55	64
15	6	1a , 2m	ND	90

^aReaction conditions: Cu (1–1.2 mol %), azide/alkyne/amine (1:1:1), room temperature, UVA irradiation. Yields were calculated by ¹H NMR analysis in CDCl_3 . ^bSee Chart 1.

Chart 1. Azides and Alkynes Included in Table 2



9 and 11). In the case of the azides studied, the catalysts proved useful toward different electronic demands, and only the aryl azide was inactive.

Finally, as shown in Figure 6, the reusability of both catalysts was tested for the reaction of **1a** and **2a** in THF in air upon

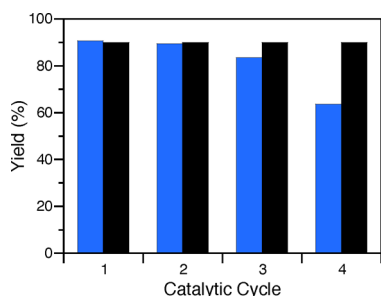


Figure 6. Reusability of CuO_x@TiO₂ (black) and CuO_x@Nb₂O₅ (blue) as per conditions in Table 2, entry 1.

UVA irradiation for 6 h, when the high-yield plateau is reached for both TiO₂- and Nb₂O₅-supported catalysts (Figure 3). We note that both catalysts showed great stability after at least four reusability cycles. This stability can be explained by the continuous regeneration of Cu(I) upon light irradiation. ICP analysis of the crude reaction mixture showed barely 0.01% and 0.002% of the available copper for the cases of CuO_x@Nb₂O₅ and CuO_x@TiO₂, respectively. These numbers suggest that the release of Cu species during the reaction is negligible, in accordance with the good performance of both catalysts during several catalytic cycles.

In summary, we have developed a new method to photocatalyze CuAAC under mild conditions with easy product isolation. We have described the use of two semiconductors as supports for copper nanoparticles, both showing excellent performance. Nb₂O₅ is a largely unexplored material that is sometimes employed as a strong acid²⁵ but rarely as a photocatalyst. In our system, the light is used to inject electrons to copper oxide from the semiconductor. The catalyst can be reused several times because of the continuous generation of Cu(I) species under excitation of the semiconductor band gap. The catalyst is moisture-tolerant and needs air and room temperature for optimal performance. The scope of the reaction demonstrates the versatility of the catalysts, extending their use to aliphatic alkynes.

■ ASSOCIATED CONTENT

📄 Supporting Information

The Supporting Information is available free of charge on the ACS Publications website at DOI: 10.1021/jacs.6b06922.

Experimental details, instrumentation used, and characterization of materials (PDF)

■ AUTHOR INFORMATION

Corresponding Authors

*titoscaiano@mac.com
 *anabel.lanterna@icloud.com
 *niejun@mail.buct.edu.cn

Author Contributions

§B.W. and J.D. contributed equally.

Notes

The authors declare no competing financial interest.

■ ACKNOWLEDGMENTS

We thank the Natural Sciences and Engineering Research Council, the Canada Foundation for Innovation, and the Canada Research Chairs Program. B.W. thanks Beijing

University of Chemical Technology for an International Joint Graduate-Training Program Scholarship.

■ REFERENCES

- (1) Rostovtsev, V. V.; Green, L. G.; Fokin, V. V.; Sharpless, K. B. *Angew. Chem., Int. Ed.* **2002**, *41*, 2596–2599.
- (2) Molteni, G.; Bianchi, C.; Marinoni, G.; Santo, N.; Ponti, A. *New J. Chem.* **2006**, *30*, 1137–1139.
- (3) Decan, M. R.; Impellizzeri, S.; Marin, M. L.; Scaiano, J. C. *Nat. Commun.* **2014**, *5*, 4612.
- (4) Davies, I. W.; Matty, L.; Hughes, D. L.; Reider, P. J. *J. Am. Chem. Soc.* **2001**, *123*, 10139–10140.
- (5) Lipshutz, B. H.; Taft, B. R. *Angew. Chem., Int. Ed.* **2006**, *45*, 8235–8238.
- (6) Decan, M. R.; Scaiano, J. C. *J. Phys. Chem. Lett.* **2015**, *6*, 4049–4053.
- (7) Arumugam, S.; Orski, S. V.; Mbua, N. E.; McNitt, C.; Boons, G.-J.; Locklin, J.; Popik, V. V. *Pure Appl. Chem.* **2013**, *85*, 1499–1513.
- (8) Tasdelen, M. A.; Yagci, Y. *Angew. Chem., Int. Ed.* **2013**, *52*, 5930–5938.
- (9) Adzima, B.; Tao, Y.; Kloxin, C.; Deforest, C.; Anseth, K.; Bowman, C. *Nat. Chem.* **2011**, *3*, 258–261.
- (10) Katayama, T.; Kamata, K.; Yamaguchi, K.; Mizuno, N. *ChemSusChem* **2009**, *2*, 59–62. Yamaguchi, K.; Oishi, T.; Katayama, T.; Mizuno, N. *Chem. - Eur. J.* **2009**, *15*, 10464–10472.
- (11) Pan, H. *Renewable Sustainable Energy Rev.* **2016**, *57*, 584–601.
- (12) Ni, M.; Leung, M. K. H.; Leung, D. Y. C.; Sumathy, K. *Renewable Sustainable Energy Rev.* **2007**, *11*, 401–425.
- (13) Hashimoto, K.; Irie, H.; Fujishima, A. *Jpn. J. Appl. Phys.* **2005**, *44*, 8269.
- (14) Chassaing, S.; Beneteau, V.; Pale, P. *Catal. Sci. Technol.* **2016**, *6*, 923–957.
- (15) Bandara, J.; Udawatta, C. P. K.; Rajapakse, C. S. K. *Photochem. Photobiol. Sci.* **2005**, *4*, 857–861.
- (16) Gomes Silva, C.; Juárez, R.; Marino, T.; Molinari, R.; Garcia, H. *J. Am. Chem. Soc.* **2011**, *133*, 595–602.
- (17) Sabio, E. M.; Chamousis, R. L.; Browning, N. D.; Osterloh, F. E. *J. Phys. Chem. C* **2012**, *116*, 19051–19051.
- (18) Hoffmann, N. *Aust. J. Chem.* **2015**, *68*, 1621–1639.
- (19) Lin, H. Y.; Yang, H. C.; Wang, W. L. *Catal. Today* **2011**, *174*, 106–113.
- (20) Scaiano, J. C.; Stampelcoskie, K. G.; Hallett-Tapley, G. L. *Chem. Commun.* **2012**, *48*, 4798–4808.
- (21) Alonso, F.; Moglie, Y.; Radivoy, G.; Yus, M. *Adv. Synth. Catal.* **2010**, *352*, 3208–3214.
- (22) Xu, L.; Yang, Y.; Hu, Z. W.; Yu, S. H. *ACS Nano* **2016**, *10*, 3823–3834.
- (23) Hein, J.; Fokin, V. *Chem. Soc. Rev.* **2010**, *39*, 1302–1315.
- (24) Meldal, M.; Tormøe, C. W. *Chem. Rev.* **2008**, *108*, 2952–3015.
- (25) Pulkkinen, P.; Shan, J.; Leppanen, K.; Kansakoski, A.; Laiho, A.; Jarn, M.; Tenhu, H. *ACS Appl. Mater. Interfaces* **2009**, *1*, 519–525.
- (26) Kulkarni, D.; Wachs, S. E. *Appl. Catal., A* **2002**, *237*, 121–137.
- (27) Tasdelen, M. A.; Yilmaz, G.; Iskin, B.; Yagci, Y. *Macromolecules* **2012**, *45*, 56–61.
- (28) Marin, M. L.; Hallett-Tapley, G. L.; Impellizzeri, S.; Fasciani, C.; Simoncelli, S.; Netto-Ferreira, J. C.; Scaiano, J. C. *Catal. Sci. Technol.* **2014**, *4*, 3044–3052.